



1 **Biogenic silica production and diatom dynamics in the Svalbard region during spring**

2

3

4 Jeffrey W. Krause^{1,2}, Carlos M. Duarte^{3,4}, Israel A. Marquez^{1,2}, Philipp Assmy⁵, Mar Fernández-
5 Méndez⁵, Ingrid Wiedmann⁶, Paul Wassmann⁶, Svein Kristiansen⁶, and Susana Agustí³,

6

7 ¹Dauphin Island Sea Lab, Dauphin Island, United States

8 ²Department of Marine Sciences, University of South Alabama, Mobile, United States

9 ³King Abdullah University of Science and Technology, Thuwal, Kingdom of Saudi Arabia

10 ⁴Arctic Research Centre, Department of Bioscience, Aarhus University, Denmark

11 ⁵Norwegian Polar Institute, Tromsø, Norway

12 ⁶Department of Arctic and Marine Biology, UiT The Arctic University of Norway, Tromsø,
13 Norway

14

15 **Correspondence:** Jeffrey Krause (jkrause@disl.edu)

16

17

18

19

20



21 **Abstract.**

22 Diatoms are generally the dominant contributors to the Arctic Ocean spring bloom, which is a key
23 event in regional food webs in terms of capacity for secondary production and organic matter
24 export. Dissolved silicic acid is an obligate nutrient for diatoms and has been declining in the
25 European Arctic. The lack of regional silicon cycling information precludes understanding the
26 consequences of such changes for diatom productivity during the Arctic spring bloom. This study
27 communicates the results from a cruise in the European Arctic around Svalbard reporting the first
28 concurrent data on biogenic silica production and export, diatom cellular export, the degree of
29 kinetic limitation by ambient silicic acid, and diatom contribution to primary production. Regional
30 biogenic silica production rates were significantly lower than those achievable in the Southern
31 Ocean and silicic acid concentration limited the biogenic silica production rate in 95% of samples.
32 Compared to diatoms in the Atlantic subtropical gyre, regional diatoms are less adapted for silicic
33 acid uptake at low substrate, and at some stations during the present study, silicon limitation may
34 have been intense enough to limit diatom growth. Thus, silicic acid can play a critical role in
35 diatom spring bloom dynamics. Diatom contribution to primary production was variable, ranging
36 from <10% to ~100% depending on the bloom stage and phytoplankton composition. While there
37 was agreement with previous studies regarding the rate of diatom cellular export, we observed
38 significantly elevated biogenic silica export. Such a discrepancy can be resolved if a higher
39 fraction of the diatom material exported during our study was modified by zooplankton grazers or
40 originated from melting ice. This study provides the most-direct evidence to date suggesting the
41 important coupling of the silicon and carbon cycles during the spring bloom in the European
42 Arctic.



43 1 Introduction

44 Diatoms and the flagellate *Phaeocystis* are the dominant contributors to the Arctic Ocean
45 spring bloom, a cornerstone event supplying much of the annual net community production
46 (Vaquer-Sunyer et al., 2013; Rat'kova and Wassmann, 2002; Wassmann et al., 1999) that fuels
47 Arctic food webs (Degerlund and Eilertsen (2010) and references therein). Hydrographic and
48 chemical changes in the Arctic water column are expected in the future, but whether these will
49 alter diatoms' contribution to spring primary production and organic matter export remains
50 uncertain. Some studies predict lack of ice cover will enhance the spring bloom due to increased
51 light availability (Arrigo et al., 2008), while others predict lower productivity driven by increased
52 stratification and reduced nutrient supply (Tremblay and Gagnon, 2009). Additionally, models
53 predict that warming will lead to a shift from a diatom-dominated bloom to one increasingly
54 dominated by flagellates and picoautotrophs, which has been observed in certain sectors of the
55 Arctic (Li et al., 2009; Lasternas and Agustí, 2010). Because the spring diatom bloom is arguably
56 the single most important productivity event for the Arctic Ocean ecosystem (Degerlund and
57 Eilertsen, 2010; Holding et al., 2015; Vaquer-Sunyer et al., 2013), understanding how diatoms'
58 ecological and biogeochemical importance changes in response to system-wide physical/chemical
59 shifts is important to predict future food web alterations. Diatoms have an obligate requirement
60 for silicon, therefore understanding of regional Si cycling can provide insights into the diatom
61 activity. However, there is a current knowledge gap of regional silicon cycling, which precludes
62 robust assessments of the spring bloom in future scenarios, e.g. Tréguer et al. (2018).

63 Diatom production is dependent on the availability of dissolved silicic acid ($\text{Si}(\text{OH})_4$),
64 which they use to build their shells of biogenic silica (bSiO_2). $[\text{Si}(\text{OH})_4]$ has been observed to be
65 low ($<5 \mu\text{M}$) in the Norwegian Seas and declining over time (Rey, 2012). A more recent analysis
66 demonstrated a decline in pre-bloom $[\text{Si}(\text{OH})_4]$ concentrations by $1\text{--}2 \mu\text{M}$ across the north Atlantic
67 subpolar and polar regions over the last 25 years (Hátún et al., 2017); this is consistent with the
68 general Arctic region being a net exporter of silicic acid (Torres-Valdés et al., 2013). This is in
69 stark contrast to the $10\text{--}60 \mu\text{M}$ $[\text{Si}(\text{OH})_4]$ observed in the surface waters of the Southern Ocean
70 and the marginal ice zone around Antarctica (Nelson and Gordon, 1982; Brzezinski et al., 2001),
71 where $[\text{Si}(\text{OH})_4]$ is unlikely to limit the rate of diatom production or biomass yield. Additionally,
72 the stoichiometry of $\text{Si}(\text{OH})_4$ availability relative to nitrate ($\text{Si:N} < 1$) in the source waters, which
73 fuel the spring bloom in most of the north Atlantic and European polar seas, suggests that during
74 a bloom cycle diatoms may experience Si limitation prior to N limitation, especially if diatoms
75 consumed Si and N in near equal quantities as in other diatom bloom regions (Brzezinski et al.,
76 1997; Brzezinski, 1985; Dugdale et al., 1995) and a $2 \mu\text{M}$ threshold $[\text{Si}(\text{OH})_4]$ defines where
77 diatoms are outcompeted by flagellates (Egge and Aksnes, 1992).

78 Compared to the Southern Ocean, there is a paucity of field Si-cycling studies in the
79 European Arctic. Reports of diatom silica production are only available from the subarctic
80 northeast Atlantic near $\sim 60^\circ \text{N}$, e.g. between Iceland and Scotland (Allen et al., 2005; Brown et
81 al., 2003), Oslofjorden (Kristiansen et al., 2000), and limited data from Baffin Bay (Hoppe et al.,
82 2018; Tremblay et al., 2002); these previous studies are in zones with higher $\text{Si}(\text{OH})_4$ availability
83 than in the European Arctic. Other studies have reported standing stocks of bSiO_2 and export in
84 Oslofjorden or the European Arctic, e.g. Svalbard vicinity, Laptev Sea (Hodal et al., 2012;
85 Heiskanen and Keck, 1996; Paasche and Ostergren, 1980; Lalande et al., 2016; Lalande et al.,
86 2013), but none have concurrent measurements of bSiO_2 production. Indeed, in the last major
87 review of the global marine silicon cycle, Tréguer and De La Rocha (2013) reported no studies
88 with published bSiO_2 production data derived from field measurements from the Arctic.



89 Currently, we lack a baseline understanding about diatom Si-cycling in the European Arctic
90 and broader high-latitude north Atlantic region. And while models in the Barents Sea use Si as a
91 possible limiting nutrient (Wassmann et al., 2006; Slagstad and Støle-Hansen, 1991), there are no
92 field data to ground truth the modeled parameters governing diatom Si uptake. Thus, there is no
93 contextual understanding to determine the consequences of the observed changes in regional
94 $[\text{Si}(\text{OH})_4]$ since the 1990s and if these affect spring bloom dynamics. This study communicates
95 the results from a cruise in the European Arctic around Svalbard reporting the first concurrent
96 datasets on regional bSiO_2 production and export, diatom cellular export, and the degree of kinetic
97 limitation by ambient $[\text{Si}(\text{OH})_4]$. Additionally, coupling bSiO_2 production rates with
98 contemporaneous primary production measurements provides an independent assessment for the
99 diatom contribution to system primary production.

100

101 **2 Methods**

102 **2.1 Region and Sampling**

103 This study was conducted aboard the RV *Helmer Hanssen* between May 17–29, 2016 as
104 part of the broader project, ARCEX–The Research Centre for ARctic Petroleum Exploration
105 (<http://www.arcex.no/>). The main goal of this cruise was to study the pelagic and benthic
106 ecosystem during the Arctic spring bloom around Svalbard and in the northern Barents Sea at
107 stations influenced by various water masses. The cruise started in the southwestern fjords
108 influenced by relatively warm Atlantic water, then transited east of Svalbard toward more Arctic-
109 influenced water (Fig. 1 blue arrow) before turning south towards stations near the Polar Front and
110 more Atlantic-water station (Fig. 1 red arrows) located to the south of the Polar Front.

111 Vertical profiles with a CTD were conducted at all stations. Hydrocasts were conducted
112 using a Seabird Electronics 911 plus CTD with an oxygen sensor, fluorometer, turbidity meter and
113 PAR sensor (Biospherical/LI-CORR, SN 1060). The CTD was surrounded by a rosette with 12
114 five-liter Niskin bottles. At two stations, Edgeøya, and Hinlopen, only surface samples were
115 collected (no vertical profiles with ancillary measurements, Fig. 1). Water was sampled from the
116 rosette at depths within the upper 40 m (i.e. the extent of the photic layer); for any incubation
117 described below, the approximate irradiance at the sample depth during collection was mimicked
118 by placing incubation bottles into a bag made of neutral density screen. Incubation bags were
119 placed in a deck board acrylic incubator cooled with continuously flowing surface seawater. At
120 Hinlopen, a block of ice was collected by hand within ~10 m of the vessel and allowed to thaw in
121 a shaded container for 24 hours at ambient air temperature. After thawing, the melted solution
122 was homogenized and treated like a water sample for measurement of biomass and rates.

123 Four sediment trap arrays were deployed between 19 and 23 hours. Arrays in van
124 Mijenfjorden and Hornsund were anchored to the bottom, whereas the other two arrays (Erik
125 Erikssenstretet, Polar Front) were quasi-Lagrangian and drifted between 14–16 km during the
126 deployment. During the Erik Erikssenstretet deployment, the array was anchored to an ice floe.
127 Arrays included sediment trap cylinders (72 mm internal diameter, 1.8 L volume; KC Denmark)
128 at 3–7 depths between 20 and 150–200 m, based on bathymetry. After recovery, trap contents
129 were pooled and subsampled for bSiO_2 and phytoplankton taxonomy.

130

131 **2.2 Standing stock measurements**

132 A suite of macronutrients were analyzed at all stations except Hinlopen (just $\text{Si}(\text{OH})_4$).
133 Water was sampled directly from the rosette, filtered (0.7 μm pore size) and immediately frozen.
134 In the laboratory, nutrients were analyzed using a Flow Solution IV analyzer (O.I. Analytical,



135 USA) and calibrated with reference seawater (Ocean Scientific International Ltd. UK). Detection
136 limits for $[\text{NO}_3 + \text{NO}_2]$ and $[\text{Si}(\text{OH})_4]$ were 0.02 and 0.07 (μM), respectively. Phosphate was
137 analyzed, but N:P ratios for nutrients were, on average, 8 among all stations, suggesting that N
138 was likely more important than P for primary production. These phosphate data are not discussed.

139 Samples for biogenic particulates and phytoplankton community composition were taken
140 directly from the rosette and sediment traps. For bSiO_2 samples, 600 mL of seawater was collected
141 from the rosette, filtered through a 1.2 μm polycarbonate filter (Millipore); for sediment trap
142 material, less volume was necessary (e.g. 50–100 mL). Most bSiO_2 protocols use a 0.6 μm filter
143 cutoff, e.g. Lalande et al. (2016), however, given the magnitude bSiO_2 quantified and the size
144 range for regional diatoms we are confident that there was no meaningful systematic
145 underestimate. After filtration, all samples were dried at 60° C and stored until laboratory analysis
146 using an alkaline digestion in Teflon tubes (Krause et al., 2009). For Chl *a*, water-column and
147 sediment samples were collected similarly, filtered on Whatman GF/F (0.7 μm pore size) and
148 immediately frozen (-20 °C). In the laboratory, Chl *a* was extracted in 5 mL methanol in the dark
149 at room temperature for 12 h. The solution was quantified using a Turner Design 10-AU
150 fluorometer, calibrated with Chl *a* standard (Sigma C6144), before and after adding two drops of
151 5% HCl (Holm-Hansen and Riemann, 1978). Phytoplankton taxonomy and abundance samples
152 were collected in 200 mL brown glass bottles from both the water column and sediment traps,
153 immediately fixed with an aldehyde mixture of hexamethylenetetramine-buffered formaldehyde
154 and glutaraldehyde at 0.1 and 1% final concentration, respectively, as suggested by Tsuji and
155 Yanagita (1981) and stored cool (5°C) and dark. Samples were analyzed with an inverted
156 epifluorescence microscope (Nikon TE300 and Ti-S, Japan), using the Utermöhl (1958) method,
157 in a service laboratory for diatom taxonomy (>90 individual genera/species categories were
158 identified) and abundance at the Institute of Oceanology Polish Academy of Science.

159

160 2.3 Rate measurements

161 Biogenic silica production was measured using the radioisotope tracer ^{32}Si . Approximately
162 150 or 300 mL samples, depending on the station biomass, were incubated with 260 Bq of high
163 specific activity $^{32}\text{Si}(\text{OH})_4$ (>20 kBq $\mu\text{mol Si}^{-1}$). After addition, samples were transported to the
164 deck-board incubator and placed in neutral density screened bags for 24 hours. After incubation,
165 samples were processed immediately by filtering bottle contents through a 25 mm, 1.2 μm
166 polycarbonate filter (Millipore) —matching bSiO_2 filtrations. Each filter was then placed on a
167 nylon planchette, covered with Mylar when completely dry, and secured using a nylon ring.
168 Samples were aged into secular equilibrium between ^{32}Si and its daughter isotope, ^{32}P (~120 days).
169 ^{32}Si activity was quantified on a GM Multicounter (Risø National Laboratory, Technical
170 University of Denmark) as described in Krause et al. (2011). A biomass-specific rate (i.e. V_b) was
171 determined by normalizing the gross rate (ρ) to the corresponding $[\text{bSiO}_2]$ at the same depth of
172 collection using a logistic-growth approach (Kristiansen et al., 2000; Krause et al., 2011). For
173 bSiO_2 and ρ , values within a profile were integrated throughout the euphotic zone (i.e. surface to
174 1% I_0) using a trapezoidal scheme. A depth-weighted V_b was calculated within the euphotic zone
175 by integrating V_b and dividing by the depth integration (Krause et al., 2013).

176 Two methods were used to assess whether ambient silicic acid ($\text{Si}(\text{OH})_4$) limited diatom Si
177 uptake. The ^{32}Si activity additions, incubation conditions, and sample processing are as described
178 above. At four stations (Edgeøya, Polar Front, Hinlopen and Atlantic), eight 300-mL samples
179 collected at a single depth within the euphotic zone and were manipulated to make an eight-point
180 concentration gradient between ambient and +18.0 μM $[\text{Si}(\text{OH})_4]$; the maximum concentration



181 was assumed to saturate Si uptake. Si uptake has been shown to conform to a rectangular
182 hyperbola described by the Michaelis-Menten equation:

$$183 \quad V_b = \frac{V_{\max}[\text{Si}(\text{OH})_4]}{K_S + [\text{Si}(\text{OH})_4]} \quad (1)$$

184 where V_{\max} is the maximum specific uptake rate and K_S is half-saturation constant, i.e.
185 concentration where $V_b = \frac{1}{2} V_{\max}$. Data were fit to the Eq. 1 using a non-linear curve fit algorithm
186 (SigmaPlot 12.3). The second type of experiment used only two points: ambient and $+18.0 \mu\text{M}$
187 $[\text{Si}(\text{OH})_4]$; four-depth profiles were done at three stations (Bellsund Hula, Hornsunddjupet, Erik
188 Erikssenstretet). The ratio of Si uptake at $+18.0 \mu\text{M}$ $[\text{Si}(\text{OH})_4]$ to Si uptake at ambient $[\text{Si}(\text{OH})_4]$
189 defines an enhancement (i.e. Enh) statistic. This two-point approach was conducted at all depths
190 in the euphotic zone; Enh ratios >1.08 imply kinetic limitation beyond analytical error given the
191 methodology (Krause et al., 2012).

192 Net primary productivity (PP) was quantified concurrently with biogenic silica production
193 at six stations at the depth of approximately 50% of surface irradiance (Table 1). Carbon uptake
194 rates were measured using a modification of the ^{14}C uptake method (Steemann Nielsen, 1952).
195 Water samples were spiked with $0.2 \mu\text{Ci mL}^{-1}$ of ^{14}C labelled sodium bicarbonate (Perkin Elmer,
196 USA) and distributed in three clear and one dark plastic bottles (40 mL each). Subsequently, they
197 were incubated for 24 h in the deck incubator with a 50% light reduction mesh. After incubation,
198 samples were filtered onto $0.2 \mu\text{m}$ nitrocellulose filters. The filters were stored frozen (-20°C) in
199 scintillation vials with 10 ml EcoLume scintillation liquid (MP Biomedicals LLC, USA) until
200 further processing. Once on land, the particulate ^{14}C was determined using a scintillation counter
201 (TriCarb 2900 TR, Perkin Elmer, USA). The carbon uptake values in the dark were subtracted
202 from the mean of the triplicate carbon uptake values measured in the light incubations. Using
203 contemporaneous ρ measurements and PP measurements, the diatom contribution to PP is
204 estimated as:

$$205 \quad \text{Diatom \%PP} = 100 \times \frac{\rho \times (\text{Si:C})^{-1}}{\text{PP}} \quad (2)$$

206 where the Si:C ratio for diatoms can be used from culture values, e.g. 0.13 (Brzezinski, 1985).

207 Export rates were calculated using the standing stock measurements, length of deployment,
208 and trap opening area. These approaches are common and detailed elsewhere (Wiedmann et al.,
209 2014; Krause et al., 2009).

210

211 **3 Results**

212 **3.1 Hydrography and Spatial patterns**

213 The regional ecosystem around Svalbard is driven by ice dynamics (Sakshaug, 2004). One
214 week prior to the cruise, a majority of the southern Svalbard archipelago had open water, which
215 was anomalous compared to similar dates in previous years (e.g. 2014, 2015, ice data archived at
216 <http://polarview.met.no/>). By the end of the cruise, Svalbard could have been entirely circled by
217 the vessel, with only open drift ice in the northeastern region. While 2016 was among the lowest
218 years for total Arctic sea ice, the ice extent in Svalbard and the Barents Sea is highly dynamic. Ice
219 edges may be pushed southward into the Barents Sea proper by wind while areas to the north
220 remain ice free, e.g. Wassmann et al. (1999) and references therein.

221 Spatial patterns in hydrography and nutrients were highly variable. In the southwestern
222 stations (e.g. fjords and Atlantic-influenced water), the surface temperature ranged between $1\text{--}4$
223 $^\circ\text{C}$; similar temperature was observed in the Atlantic station south of the Polar Front (Fig. 1E).
224 Northeastern domain stations were more influenced by Arctic water and the surface temperatures
225 ranged between $-2\text{--}1^\circ\text{C}$ (Fig. 1E). Surface nutrient concentrations, particularly $[\text{NO}_3 + \text{NO}_2]$ and



226 [Si(OH)₄], showed a broad range. The highest surface [NO₃+NO₂] was observed in the
227 southwestern fjords, 2–8 μM, and the Atlantic station (~3 μM, Fig. 1A). The surface
228 concentrations at the remaining stations were <0.5 μM or near detection limits (Fig. 1A).
229 [Si(OH)₄] was lower than [NO₃+NO₂] (i.e. Si:N <1) among stations where [NO₃+NO₂] was > 0.1
230 μM. At high [NO₃+NO₂] stations, the [Si(OH)₄] ranged from 1.1–4.5 μM (Fig. 1B) but the range
231 was lower among other stations (0.4–1.1 μM, Fig. 1B). bSiO₂ (proxy for diatom biomass, Fig.
232 1C) was typically similar to, or lower than, surface [Si(OH)₄]. The highest surface [bSiO₂] was
233 observed in the southern stations (Atlantic-influenced waters), ~ 2–3 μmol Si L⁻¹ (Fig. 1C). At
234 most other stations the [bSiO₂] was <1 μmol Si L⁻¹. Among all stations/depths bSiO₂ varied by a
235 factor of ~40 (does not include Hinlopen ice algae).

236 Primary productivity, measured at six stations at 5 m (approximately 50% of surface
237 irradiance), varied over two orders of magnitude. The lowest rates were observed at the four
238 stations having lowest surface [NO₃+NO₂] and ranged from 2–13 μg C L⁻¹ d⁻¹; at these stations
239 [Chl *a*] ranged from 2.0–4.8 μg L⁻¹ (Table 1, Fig. 1D). The highest rates were measured at van
240 Mijenfjorden and Bredjupet, 100 ±65 μg C L⁻¹ d⁻¹ and 27 ±1 μg C L⁻¹ d⁻¹, respectively, and
241 corresponded to high [NO₃+NO₂] and low [Chl *a*] 1.8 and 0.7 μg L⁻¹, respectively (Table 1, Fig.
242 1D).

243

244

245 3.2 Vertical profiles

246 As expected, most stations showed strong vertical gradients in nutrient concentrations.
247 Profiles in the southwestern region of Svalbard (van Mijenfjorden, Bredjupet) had elevated
248 [Si(OH)₄], with little vertical structure. Vertical [Si(OH)₄] profiles among other stations showed
249 typical nutrient drawdown between the surface and ~20 m. At these stations, surface [Si(OH)₄]
250 concentrations were typically <1.5 μM and subsurface values (to 20 m) ranged from 0.5–3.0 μM
251 (Fig. 2A). [NO₃+NO₂] exceeded [Si(OH)₄] among all depths at five stations (van Mijenfjorden,
252 Bredjupet, Hornsund, Atlantic; Fig. 2B), whereas in the remaining stations [NO₃+NO₂] exceeded
253 [Si(OH)₄] (i.e. Si:N <1) at depths >5 m (Bellsund Hula), >20 m (Erik Erikssenstretet) and >27 m
254 (Polar Front). For the latter three stations, [NO₃+NO₂] had a significant drawdown in surface
255 waters, but then increased with depth without a similar degree of vertical enhancement in
256 [Si(OH)₄] (Fig. 2).

257 [bSiO₂] was typically highest at or near the surface, with a maximum of ~2 μmol Si L⁻¹
258 (Fig. 2C). At the Bellsund Hula and Erik Erikssenstretet stations, subsurface [bSiO₂] maxima were
259 present (Fig. 2C; note—no surface data are available for van Mijenfjorden). Among non-profile
260 stations, [bSiO₂] was within the range observed among vertical profiles except for the Hinlopen
261 ice algae, where the melt water had exceptionally high [bSiO₂] (Fig. 2C). The surface-to-20-m
262 integrated bSiO₂ (∫bSiO₂) spanned over an order of magnitude, with a low at Bredjupet (1.9 mmol
263 Si m⁻²) and a high at Hornsunddjupet (42.4 mmol Si m⁻², Table 1) despite their proximity (~50
264 km).

265 Diatom abundance and taxonomy data were sampled at fewer stations, but the vertical and
266 spatial variability generally mirrored trends in [bSiO₂]. In the surface waters of van Mijenfjorden
267 and Hornsund, diatom abundances ranged between 5x10⁴–5x10⁵ cells L⁻¹ in the upper 50 m (Fig.
268 3A). However, within the same vertical layer at the Erik Erikssenstretet and Polar Front (duplicate
269 profiles) stations, diatom abundances were enhanced by up to two orders of magnitude (4x10⁴–
270 4x10⁷ cells L⁻¹, Fig. 3A). When integrated to 40-m depth (∫Diatom), matching the shallowest
271 sediment-trap depth among the three stations reported (Fig. 3E–H), diatom inventories also



272 showed a two-order of magnitude variability as observed in $\int \text{bSiO}_2$. $\int \text{Diatom}$ was lowest at van
273 Mijenfjorden (7.67×10^9 cells m^{-2}) and highest at Polar Front station (527×10^9 cells m^{-2} , Table 1).

274 Among the stations which had corresponding sediment trap deployments (van
275 Mijenfjorden, Hornsund, Erik Erikssenstretet), the diatom-assembly composition was similar
276 despite differences in abundance. The van Mijenfjorden station was dominated by *Thalassiosira*
277 (e.g. *T. antarctica*, *T. gravida*, *T. hyalina*, *T. nordenskiöldii*), *Fragilariopsis cylindrus*, and
278 *Chaetoceros furcellatus* (Fig. 3B). *Chaetoceros* spp. was nearly absent from Erik Erikssenstretet
279 (Fig. 3D) and of little importance at Hornsund (Fig. 3C). *Thalassiosira* species (same as van
280 Mijenfjorden) cells also dominated Hornsund and Erik Erikssenstretet among most depths (Fig.
281 3C, D). However, at Hornsund, deeper depths were dominated by diatom groups less frequently
282 observed (“Other diatom” category, Fig. 3), and with small contributions from *Fragilariopsis*
283 *cylindrus* and *Navicula vanhoefenii*.

284 Diatom bSiO_2 productivity, ρ , mirrored trends in biomass. Among the profiles, rates
285 generally varied from $\rho < 0.01$ to $0.11 \mu\text{mol Si L}^{-1} \text{d}^{-1}$ (Fig. 2D). ρ was highest in the Atlantic
286 station (Fig. 2D), which was expected given the higher bSiO_2 (Fig. 2C). However, the rates in the
287 Hinlopen ice algae were like those quantified at Hornsunddjupet, $\sim 0.1 \mu\text{mol Si L}^{-1} \text{d}^{-1}$, despite the
288 ice algae station having an order of magnitude more biomass. This suggests the Hinlopen ice algae
289 were senescent or stressed and a sizable portion of the measured bSiO_2 was non-active or detrital.
290 When integrated in the upper 20-m, $\int \rho$ ranged from $0.27 - 1.46 \text{ mmol Si m}^{-2} \text{d}^{-1}$ (Table 1), which
291 is a smaller proportional range than observed in $\int \text{Diatoms}$ and $\int \text{bSiO}_2$. Overall, bSiO_2 -normalized
292 rates (V_b) were low among all stations and depths (< 0.01 to 0.13 d^{-1}). The depth-weighted V_b , i.e.
293 V_{AVE} , had a narrower range between $0.03 - 0.13 \text{ d}^{-1}$. Thus, doubling times for bSiO_2 in the upper
294 20 m ranged between 5–23 days.

295 The rate of diatom biogenic silica production was reduced by ambient $[\text{Si}(\text{OH})_4]$ in 95% of
296 the samples examined. Full kinetic experiments verified that Si uptake conformed to Michaelis-
297 Menten kinetics (Fig. 4A; adjusted R^2 ranged $0.64 - 0.92$ among experiments). The highest V_{max}
298 was observed in the Atlantic station ($0.36 \pm 0.02 \text{ d}^{-1}$), which also had the highest ambient $[\text{Si}(\text{OH})_4]$
299 among the full kinetic experiments ($1.4 \mu\text{M}$). V_{max} observed at Edgeøya and the Polar Front were
300 nearly identical ($0.05 \pm < 0.01 \text{ d}^{-1}$ for both) and lowest in the Hinlopen ice diatoms ($0.02 \pm < 0.01 \text{ d}^{-1}$).
301 K_S constants had a narrower range, with a low of $0.8 \pm 0.3 \mu\text{M}$ at the Polar Front and between
302 $2.1 - 2.5 \mu\text{M}$ among the other three stations. Among these full-kinetic experiments, the Enh ratio
303 ranged from $1.8 - 7.7$ with the most intense $[\text{Si}(\text{OH})_4]$ limitation of uptake observed in the Hinlopen
304 ice diatoms. For profiles where two-point kinetic experiments were conducted, the same trends
305 were observed (Fig. 4B). The Enh ratio was similar among depths at Bellsund Hula ($1.5 - 2.2$),
306 Hornsunddjupet and Bredjupet ($3.4 - 5.4$ for latter two stations, Fig. 4B). At Erik Erikssenstretet,
307 Enh ratios were more variable, ranging from $2.8 - 7.3$ in the upper 10 m with no Enh effect (i.e.
308 < 1.08) observed at 20 m —this was the only sample and depth which showed no resolvable degree
309 of kinetic limitation for Si uptake.

310 Rates of bSiO_2 - and diatom export were variable. Among the three sediment trap regions,
311 bSiO_2 export rates ranged from $\sim 4 - 10 \text{ mmol Si m}^{-2} \text{d}^{-1}$ (Fig. 2E). These rates are significant and
312 represent up to 50% of the $\int \text{bSiO}_2$ in upper 20 m at van Mijenfjorden (Table 1). For diatom cells,
313 a similar degree of variability was observed. Export at van Mijenfjorden ranged from $390 - 1500$
314 $\times 10^6$ cells $\text{m}^{-2} \text{d}^{-1}$, similar ranges to Hornsund ($520 - 2800 \times 10^6$ cells $\text{m}^{-2} \text{d}^{-1}$) and Erik Erikssenstretet
315 ($510 - 860 \times 10^6$ cells $\text{m}^{-2} \text{d}^{-1}$, Fig. 3E). The Atlantic station had significantly higher diatom export
316 ($800 - 2300 \times 10^6$ cells $\text{m}^{-2} \text{d}^{-1}$) among all depths in the upper 120 m (Fig. 3E). The bSiO_2 and
317 diatom cellular export were highly correlated ($r = 0.67$, $p < 0.01$; Spearman’s Rho Test). Among



318 all stations, *Fragilariopsis cylindrus* had the highest contribution to diatom export, and
319 *Thalassiosira* species (e.g. *T. antarctica*, *T. gravida*, *T. hyalina*, *T. nordenskioeldii*) were also
320 important (Fig. 3F–H). In Hornsund, *Navicula* (*N. vanhoefenii*, *N. sp.*) was an important group for
321 export (Fig. 3G) but this was not observed elsewhere. Similarly, “Other diatom” groups were
322 proportionally important at Erik Erikssenstretet (Fig. 3H), as were *Thalassiosira* resting spores at
323 the Atlantic station (data not shown). Among all diatoms, the only groups which were numerically
324 important in both the water column and the sediment traps were *Fragilariopsis cylindrus* and
325 *Thalassiosira* species (Fig. 3B–D, F–H).

326

327 4 Discussion

328 4.1 Diatom Si cycling relative to other systems

329 To our knowledge, this is the first report of bSiO₂ production data of the natural diatom
330 community in this sector of the Arctic. Other studies have reported ρ data in the subarctic Atlantic
331 Ocean (Brown et al., 2003; Kristiansen et al., 2000; Allen et al., 2005) ~10–20° latitude south of
332 our study region or in Baffin Bay (Hoppe et al., 2018; Tremblay et al., 2002). However, the Hoppe
333 et al. (2018) study only includes ρ measured after a 24-hour manipulation experiment and only at
334 one site and depth near the Clyde River just east of Nunavut (Canada), no data are reported for the
335 ambient conditions, and the measurements from Tremblay et al. (2002) are based on net changes
336 in standing stocks instead of gross bSiO₂ production. Banahan and Goering (1986) report the only
337 ρ to date in the southeastern Bering Sea; however, Varela et al. (2013) recently reported that
338 [Si(OH)₄] in surface waters (>5 μM) are unlikely to be significantly limiting to diatoms in any
339 sector of the Bering, Chukchi or Beaufort Sea regions. Around Svalbard, some previous studies
340 have examined other Si-cycling components including variability in bSiO₂ in the water column
341 (Hodal et al., 2012) and sediments (Hulth et al., 1996), bSiO₂ and diatom export (Lalande et al.,
342 2016; Lalande et al., 2013), or trends in [Si(OH)₄] (Anderson and Dryssen, 1981). The ρ
343 measurements presented here have no straight forward study for comparison; therefore, we
344 compare these to the previous high-latitude Atlantic data and to well-studied sectors of the
345 Southern Ocean.

346 During our study, $\int\rho$ in the Svalbard vicinity was low. Working in the NE Atlantic between
347 Iceland and Scotland, Brown et al. (2003) reported $\int\rho$ between 6–166 mmol Si m⁻² d⁻¹. In the same
348 region, under post-bloom conditions, Allen et al. (2005) reported 7 mmol Si m⁻² d⁻¹ for one profile.
349 These rates are significantly higher than at our four profile stations (Table 1), and the degree of
350 difference does not appear to be driven by differences in integration depth (compared to our study,
351 Table 1). Given the higher [Si(OH)₄] in the southern region of the Atlantic subpolar gyre (Hátún
352 et al., 2017), the maximum achievable $\int\rho$ may vary with latitude. While our profile sampling was
353 opportunistic, it appears we sampled some stations with significant diatom biomass (high $\int\text{bSiO}_2$),
354 but the corresponding production rates ($\int\rho$) were low, with estimated doubling times on the order
355 of 11–23 days. This suggests these high-biomass stations may have been near, or past, peak bloom
356 conditions (Fig. 2A, B) and the seasonal timing is consistent with regional field and modeling
357 studies inferring diatom bloom dynamics from Chl *a* trends, e.g. (Wassmann et al., 2010; Oziel
358 et al., 2017). Kristiansen et al. (2000) reported ρ in Oslofjorden during the late winter (February–
359 March), rates ranged from 0.03–2.0 $\mu\text{mol Si L}^{-1}$ over nine sampling periods with corresponding
360 V_b between <0.01–0.28 d⁻¹; however, this system has a higher Si(OH)₄ supply and surface
361 concentrations at the start of the bloom period were >6 μM , approximately 50% higher than the
362 highest surface concentrations observed during our study (Fig. 2A). Nearly all the initial Si(OH)₄
363 was eventually converted to bSiO₂ during the bloom (Kristiansen et al., 2001; Kristiansen et al.,



364 2000). The specific rates observed in our study fall within the lower values reported by Kristiansen
365 et al. (2000), which may be explained by the reduced uptake from lower $[\text{Si}(\text{OH})_4]$ (e.g. Fig. 4).

366 The Southern Ocean is one of the most globally significant regions for production of bSiO_2 .
367 The surface $[\text{Si}(\text{OH})_4]$ and $[\text{NO}_3+\text{NO}_2]$ are among the highest in the ocean and the source waters
368 usually have >50% excess $\text{Si}(\text{OH})_4$ relative to nitrate (Brzezinski et al., 2002). Thus, exceptional
369 $\text{Si}(\text{OH})_4$ drawdown relative to nitrate is required for diatom biomass yield to be limited by Si in
370 this region. The mean $\int \rho$ in sectors of the Southern Ocean are variable. In the Weddell Sea, winter
371 rates range between 2.0–3.2 $\text{mmol Si m}^{-2} \text{d}^{-1}$ in the seasonal ice zone (Leynaert et al., 1993).
372 Within the sub-Antarctic zone, rates averaged 1.1 and 4.8 $\text{mmol Si m}^{-2} \text{d}^{-1}$ in the summer and
373 spring, respectively (Fripiat et al., 2011). At the terminus of diatom blooms in the sub-Antarctic
374 and polar frontal zone, rates can be lower, e.g. 0.1–0.3 $\text{mmol Si m}^{-2} \text{d}^{-1}$ (Fripiat et al., 2011); such
375 values are similar to the range observed during our study, especially since these Southern Ocean
376 studies integrated $\int \rho$ deeper than 40 m (e.g. 50–100 m). Brzezinski et al. (2001) reported average
377 $\int \rho \sim 25 \text{ mmol Si m}^{-2} \text{d}^{-1}$ (integrated from surface to 80–120 m) during intense blooms in the seasonal
378 ice zone which propagated south of the Antarctic polar front. But despite the massive diatom bSiO_2
379 accumulating in these blooms, V_{AVE} generally ranged between 0.05–0.15 d^{-1} (Brzezinski et al.,
380 2001). Given the order-of-magnitude difference in $[\text{Si}(\text{OH})_4]$ and $\int \rho$ between the Arctic and
381 Southern Ocean, the similar V_{AVE} in both regions may be more reflective of thermal effects on
382 diatom growth rate, since Si uptake and diatom growth rates are tightly coupled, or a significant
383 accumulation of detrital bSiO_2 (i.e. diatom fragments) in the Southern Ocean, where low
384 temperatures reduce bSiO_2 remineralization rates (Bidle et al., 2002).

385

386 4.2 Potential for Silicon limitation of diatom productivity

387 Suboptimal silicon availability affects the rate of diatom bSiO_2 production and can limit
388 their growth. A widely cited $[\text{Si}(\text{OH})_4]$ threshold, below which diatoms will be outcompeted by
389 other phytoplankton, is $\sim 2.0 \mu\text{M}$; this metric was derived from a comparison of diatom abundance
390 (relative to total microplankton) versus $[\text{Si}(\text{OH})_4]$ during mesocosm experiments in a Norwegian
391 fjord system (Egge and Aksnes, 1992). Applying this metric globally has been criticized due to
392 observation of diatom dominance among microplankton when $[\text{Si}(\text{OH})_4] < 1 \mu\text{M}$ in systems
393 ranging from fjords to the open-ocean (Krause et al., 2013; Hodal et al., 2012; Kristiansen et al.,
394 2001) and also culture studies showing some diatom species can maintain high growth rates when
395 $[\text{Si}(\text{OH})_4] < 0.5 \mu\text{M}$ (reviewed by Kristiansen and Hoell (2002)). Stoichiometry of silicon
396 availability relative to nitrate also help diagnose Si limitation; the most widely accepted diatom
397 Si:N ratio is ~ 1 based on temperate and low-latitude clones (Brzezinski, 1985). There is a paucity
398 of diatom culture studies examining stoichiometry in polar diatoms, but Si:N during spring blooms
399 in Oslofjorden are close to Brzezinski's Si:N ratio (Kristiansen et al., 2001). For diatoms in
400 Svalbard and the broader region of the subpolar and polar European Atlantic, both $[\text{Si}(\text{OH})_4]$ and
401 its availability relative to N appear to be suboptimal for creating intense diatom blooms, such as
402 those occurring in the Southern Ocean. Yet, the Arctic spring bloom is consistently dominated by
403 diatoms or *Phaeocystis* (Degerlund and Eilertsen, 2010), which suggests some level of adaptation
404 for diatoms to the low $[\text{Si}(\text{OH})_4]$ environment of the region.

405 Nutrient relationships support the potential for silicon to be a controlling factor of regional
406 diatom productivity. When plotting $[\text{NO}_3+\text{NO}_2]$ as a function of $[\text{Si}(\text{OH})_4]$ (Fig. 5A) a few trends
407 emerge: 1) The slope of the linear regression relationship ($2.5 \pm 0.1 \text{ mol N (mol Si)}^{-1}$) denotes that
408 NO_3+NO_2 is consumed at over twice the rate per unit $\text{Si}(\text{OH})_4$. 2) Given that the source water
409 $[\text{NO}_3+\text{NO}_2]$ concentration is only \sim twice that of $[\text{Si}(\text{OH})_4]$, a 2.5 drawdown ratio would predict



410 NO_3+NO_2 to be depleted before $\text{Si}(\text{OH})_4$. This indeed indicates that phytoplankton can deplete
411 nitrogen to levels below detection while they appear unable to deplete $\text{Si}(\text{OH})_4$ pools below 0.5
412 μM , which would indicate 0.5 μM is the ultimate $\text{Si}(\text{OH})_4$ concentration required to support diatom
413 growth. Nitrate and silicic acid drawdown within the upper 50 m during the spring season (1980–
414 1984) was discussed by Rey et al. (1987) who suggested apparent nitrate limitation (1980, 1981)
415 and silicic acid limitation (1983, 1984) are annually variable. The Reigstad et al. (2002) analysis
416 of nitrate and silicic acid drawdown in the central Barents Sea shows similarities in that the diatom
417 assemblage could only drawdown $[\text{Si}(\text{OH})_4]$ to $\sim 1 \mu\text{M}$ (May 1998) and $\sim 0.5 \mu\text{M}$ (July 1999).
418 These authors suggest that physical effects on phytoplankton explain the interannual variability in
419 the maximum $[\text{Si}(\text{OH})_4]$ drawdown, where diatoms dominate in shallow mixed waters opposed to
420 *Phaeocystis pouchetii* dominating in deeper mixed waters.

421 None of these nitrate and silicic acid relationships capture the progressive dynamics of an
422 active diatom bloom. Using the ARCEX data (Fig. 5A), if diatoms are limited by an absolute
423 $[\text{Si}(\text{OH})_4]$ (e.g. 2 μM), then at this concentration there is still ample residual $[\text{NO}_3+\text{NO}_2]$ (3.8 μM)
424 which could be used by other phytoplankton that do not consume Si (Fig. 5A). Even if the diatom
425 $[\text{Si}(\text{OH})_4]$ threshold is closer to 1 μM , this observation of excess $[\text{NO}_3+\text{NO}_2]$ (1.4 μM) still holds.
426 Diatoms have an *r*-selected ecological strategy and are typically the first phytoplankton group to
427 bloom in this region under stratified shallow-mixed conditions (Reigstad et al., 2002). If they
428 consumed N and Si in near equal amounts (i.e. Si:N ~ 1) without significant competition for N by
429 other major phytoplankton groups, it is highly probable that Si would limit them first during a
430 bloom. Clearly, interannual and local differences in mixing, which may favor *Phaeocystis*
431 *pouchetii* over diatoms (Reigstad et al., 2002), can affect the assemblage and nutrient drawdown
432 trajectory (e.g. see points with high $[\text{Si}(\text{OH})_4]$ and little measurable $[\text{NO}_3+\text{NO}_2]$, Fig. 5A);
433 therefore, diagnosing whether Si could limit diatom growth requires additional analyses.

434 When considering the European sector of the Arctic/sub-Arctic between 60°–80° N, there
435 is compelling evidence that $[\text{Si}(\text{OH})_4]$ limits the rate of diatom bSiO_2 production. During ARCEX,
436 the relationship between V_b and $[\text{Si}(\text{OH})_4]$ also supports that Si regulates diatom productivity to
437 some degree. Our kinetic data demonstrate that in three of four experiments K_S was $\sim 2.0 \mu\text{M}$, but
438 in the Polar Front the K_S was lower $\sim 0.8 \mu\text{M}$. These data are consistent with community kinetic
439 experiments reported in Oslofjorden where K_S and V_{max} were between 1.7–11.5 μM and 0.16–0.64
440 d^{-1} , respectively, with the lowest V_{max} observed during the declining diatom bloom (Kristiansen et
441 al., 2000). These authors concluded that silicon ultimately controlled diatom productivity during
442 this bloom (Kristiansen et al., 2001). In the only other kinetic experiment reported in the northeast
443 Atlantic, Allen et al. (2005) observed a linear response in V_b between ambient and 5 μM $[\text{Si}(\text{OH})_4]$,
444 which suggests uptake did not show any degree of saturation at this concentration. These field-
445 based K_S values are considerably higher than parameters used in Barents Sea models, e.g. 0.5 μM
446 (Slagstad and Støle-Hansen, 1991), 0.05 μM (Wassmann et al., 2006) which reflect the high
447 efficiency uptake seen in culture (Paasche, 1975). Fitting a regression to the $V_b V_{\text{max}}^{-1}$ as a function
448 of $[\text{Si}(\text{OH})_4]$ (line shown in Fig. 5B) suggests that 2.3 μM is the best constrained half-saturation
449 concentration (i.e. concentration where $V_b V_{\text{max}}^{-1} = 0.5$) for the regional assemblage; however, this
450 is biased from the Hornsunddjupet assemblage (white symbols, Fig. 5B), and this aggregated half-
451 saturation would increase to 2.8 μM if those data were not considered. Unlike diatoms in the north
452 Atlantic Subtropical Gyre, e.g. Sargasso Sea (Krause et al., 2012), regional diatoms do not appear
453 well-adapted for maintaining $V_b V_{\text{max}}^{-1} > 0.5$ at low $[\text{Si}(\text{OH})_4]$. Instead, diatoms during the spring
454 season appear to be best adapted for concentrations exceeding 2.3 μM , which suggests that as
455 $[\text{Si}(\text{OH})_4]$ is depleted diatoms may slow growth (Fig. 5B).



456 To avoid growth limitation, diatoms can reduce their silicon per cell when $[\text{Si}(\text{OH})_4]$ is
457 suboptimal. An accepted principal from culture work is that diatoms can alter their silicon per cell
458 by a factor of four (Martin-Jézéquel et al., 2000). Thus, when uptake is reduced to $<25\%$ of V_{max} ,
459 diatoms must slow growth to take up enough Si to produce a new cell. Using the empirical half-
460 saturation constant range (2.3–2.8 μM) calculated from Fig. 5B and using Eq. 1 to solve for the
461 concentrations where $V_b V_{\text{max}}^{-1} \leq 0.25$ (V_{max} is a constant), suggests that when $[\text{Si}(\text{OH})_4]$ is below
462 0.3–0.8 μM , the degree of kinetic limitation could force diatoms to slow growth in response. Such
463 a range could be biased low given the influence of the highly efficient Hornsunddjupet assemblage
464 (which was associated with warmer Atlantic waters). But at these $[\text{Si}(\text{OH})_4]$ there would also be
465 up to 0.8 μM $[\text{NO}_3 + \text{NO}_2]$ remaining (Fig. 5A). Therefore, under shallow stratified conditions
466 which favor diatoms over *Phaeocystis* (*sensu* Reigstad et al. (2002)), $[\text{Si}(\text{OH})_4]$ may regulate
467 regional diatom productivity during spring consistent with similar results from southern-Norway
468 fjords (Kristiansen et al., 2001). This provides the most direct assessment to date supporting the
469 general idea that Si may limit regional diatom productivity (Rey, 2012; Rey et al., 1987; Reigstad
470 et al., 2002).

471

472 **4.3 Diatom contribution to primary production**

473

474 Among the six sites with paired PP and ρ measurements, the bloom phase can be inferred
475 from the magnitude of nutrient drawdown, $[\text{Chl } a]$, PP, and pCO_2 (data not shown). Bredjupet
476 appeared to be a pre-bloom station given the nutrients, while the van Mijenfjorden station also
477 appeared to be in an early bloom phase. The Erik Erikssenstretet station represented a peak bloom
478 condition, whereas assemblages at Hornsunddjupet and Edgeøya appeared to be post bloom and
479 in a stage of decline. The Polar Front station represented the end or late-phase bloom condition;
480 however, at this station *Phaeocystis* was abundant (data not shown), suggesting it may have
481 dominated the bloom dynamics instead of diatoms.

482

483 The diatom contribution to PP was highly variable. Among the stations with high $[\text{NO}_3 +$
484 $\text{NO}_2]$ (van Mijenfjorden, Bredjupet) the diatom contribution to PP (e.g. Eq. 2) was low, 5–6%. At
485 two stations, Hornsunddjupet and the Polar Front, the diatom contribution to PP increased to 48–
486 57%. In the Edgeøya, and Erik Erikssenstretet stations, diatoms accounted for all PP, 130 and
487 340%, respectively. Such unrealistic value at Erik Erikssenstretet could imply a potential issue
488 with the Si:C ratio (Eq. 2), specifically an increase in Si per cell and/or lower C per cell due to
489 reduced growth rate associated with the peak/end of the bloom.

489

490 Clearly, diatoms can play a significant role in local productivity, but these data demonstrate
491 a “bloom and bust” nature. At stations at or near peak bloom levels (e.g. Edgeøya, Erik
492 Erikssenstretet), diatoms could account for nearly all primary production. However, they may also
493 conduct an insignificant percentage of primary production prior to the onset of the bloom (e.g. van
494 Mijenfjorden, Bredjupet). But even when physical conditions may favor *Phaeocystis* blooms,
495 diatoms appear to be significant contributors to primary production (Polar Front station). In such
496 a situation, N would be predicted to be the limiting nutrient as it will be consumed by both
497 *Phaeocystis* and diatoms whereas Si will only be consumed by the latter.

498

499 In the European Arctic, shifts in summer-period phytoplankton communities away from
500 diatom-dominated conditions have been observed in numerous studies. One of the dominant
501 features has been the increasing abundances of *Phaeocystis* in ice-edge (Lasternas and Agustí,
2010) or under-ice blooms (Assmy et al., 2017). These changes have corresponded with larger-
scale shifts in the export of diatoms to depth in the Fram Straight (Nöthig et al., 2015; Lalande et
al., 2013; Bauerfeind et al., 2009). The timing of these shifts, e.g. mid-2000s, correspond with the



502 broader regional reduction in winter mixed-layer $[\text{Si}(\text{OH})_4]$ concurrent with the shift to negative
503 gyre-index state in the latter half of the decade (Hátún et al., 2017). With a reduction in pre-bloom
504 $\text{Si}(\text{OH})_4$ supply, diatoms may run into limitation sooner and thus leave more residual nitrate for
505 non-diatom phytoplankton. Degerlund and Eilertsen (2010) also demonstrate a dynamic
506 temperature niche for individual diatom groups/species. Coello-Camba et al. (2015) showed that
507 temperature induced a shift in the Arctic phytoplankton community, with diatoms declining as
508 temperature increased and thereby favoring dominance of flagellates. Given the highly variable
509 contribution of diatoms to primary productivity in this system in spring and the effects which carry
510 over into summer, should climate change or natural physical oscillations affect diatoms in this
511 system, resolving such a signal will be challenging. A similar conclusion about detecting a
512 climate-change signal was made in the eastern Bering Sea by Lomas et al. (2012) given the natural
513 variability in primary production.

514

515 4.4 Diatoms and export

516 The bSiO_2 export rates observed during ARCEX were significant relative to the standing
517 stocks. At van Mijenfjorden, the rate of export in the upper 40 m represented 39% of the $\int \text{bSiO}_2$
518 standing stock ($23.3 \text{ mmol Si m}^{-2}$) in the same vertical layer. This quantity was much higher than
519 at Erik Erikssenstretet, where the 40-m export rate was <11% of the $\int \text{bSiO}_2$ in the upper water
520 column (note: no samples were taken deeper than 20 m, thus, additional bSiO_2 between 20–40 m
521 would lower the 11% estimate). Given that the van Mijenfjorden site was located within shallow
522 fjord waters (bottom depth approximately 60 m), such a high proportion export relative to standing
523 stock may suggest either lateral focusing processes (e.g. discussed by DeMaster (2002)) and/or
524 resuspension of sediment bSiO_2 into the water and resettlement. The rate of bSiO_2 export was also
525 at least a factor of four higher than $\int \rho$ in the upper 20 m. It is likely that some fraction of $\int \rho$ was
526 missed due to lack of sampling between 20–40 m, but with a lack of light at these depths, it is
527 unlikely systematic underestimates of ρ caused the disparity. Given the deeper water at the Erik
528 Erikssenstretet and Atlantic stations, such high bSiO_2 export may be driven by previously high ρ
529 and bSiO_2 standing stock which accumulated in the overlying waters or, given the dynamic
530 circulation in the region, this signal may have been laterally advected to these station locations.

531 Relative to previous studies, the bSiO_2 export rates were also high. During May 2012 in
532 Kongsfjorden, Lalande et al. (2016) reported bSiO_2 export rates between $0.2\text{--}1.3 \text{ mmol Si m}^{-2} \text{ d}^{-1}$
533 in the upper 100 m, a similar range was observed by Lalande et al. (2013) in the eastern Fram
534 Strait using moored sediment traps (2002–2008) collecting at depths between 180–280 m. Lalande
535 et al. (2013) concluded that, despite warm anomaly conditions, pulses of bSiO_2 export were
536 positively correlated to the presence of ice in the overlying waters which stratifies the water and
537 helps initiate a diatom bloom. However, if the light was insufficient to stimulate a bloom, Lalande
538 et al. (2013) suggested much of the pulse of bSiO_2 exported to depth may have originated in the
539 ice and sank during melting. Indeed, the low V_b ($<0.01 \text{ d}^{-1}$) observed at the Hinlopen station (ice
540 algae), despite the moderate ρ measured ($0.12 \text{ } \mu\text{mol Si L}^{-1} \text{ d}^{-1}$), suggests that most of the ice-
541 associated bSiO_2 was detrital and not associated with living diatoms. Thus, the recent ice retreat
542 observed prior to the ARCEX cruise was a potential source of such high bSiO_2 export to depth
543 despite the considerably lower $\int \rho$ in the upper 20 m.

544 Among the groups examined, the most important diatom genera for standing stock and
545 export were *Thalassiosira* and *Fragilariopsis*, suggesting these groups are important drivers of
546 bulk bSiO_2 fluxes. Given the large-size and chain-forming life histories for the dominant species
547 within each genus, it is likely that their dominance in the trap abundances helps explain the high



548 correlation ($r = 0.67$, $p < 0.01$; Spearman's Rho Test) between bSiO_2 and diatom export. Given this
549 degree of correlation, it would be expected that both bSiO_2 and diatom export would be similarly
550 enhanced relative to previous studies; however, this was not observed. Diatom cellular export in
551 Kongsfjorden (Lalande et al., 2016) were similar-to or a factor of three lower than rates quantified
552 during ARCEX (Table 1, Fig. 3E), whereas bSiO_2 export during ARCEX was over an order of
553 magnitude higher than bSiO_2 export in Kongsfjorden. One possible explanation for the higher
554 degree of bSiO_2 export enhancement, relative to diatom cellular export, between studies is that
555 more exported material during ARCEX was modified in the food web. For instance, in Erik
556 Erikssenstretet gel traps confirm the presence of aggregates and mesozooplankton fecal pellets
557 (Wiedmann et al. in prep), and in van Mijenfjorden detrital particles were most prominent on the
558 gel traps opposed to clearly recognizable material (e.g. diatom valves). These observations suggest
559 the potential for considerable modification of diatom organic matter prior to export (diatoms in
560 fecal pellets, fragments associated with aggregates, etc.). This is consistent with previous
561 observation in the Barents Sea showing high potential for copepod fecal pellets to be exported in
562 the Polar Front and Arctic-influenced regions during spring (Wexels Riser et al., 2002). And
563 supports the general ideas for the importance of diatom organic matter in fueling secondary
564 production regionally during this season (Degerlund and Eilertsen (2010) and references therein).

565

566 4.5 Conclusion

567 This is the first regional data set with contemporaneous measurements of diatom bSiO_2
568 standing stock, production, export and assessment of kinetic limitation by $[\text{Si}(\text{OH})_4]$ in the
569 European Arctic. Among stations and depths there was widespread limitation of diatom bSiO_2
570 production rates by ambient $[\text{Si}(\text{OH})_4]$ during spring-bloom conditions. The kinetic parameters
571 for diatom Si uptake (e.g. K_S) quantified in our study are significantly higher than rates used in
572 regional models and quantified in polar diatom cultures; therefore, these data will help future
573 modeling efforts better simulate diatom/Si dynamics. Given the trajectories of Si and N
574 consumption, diatom-dominated blooms (vs. *Phaeocystis*-dominated) could deplete $\text{Si}(\text{OH})_4$ prior
575 to nitrate; and at some stations, the degree of kinetic limitation by ambient $[\text{Si}(\text{OH})_4]$ could have
576 resulted in diatom growth being slowed. Diatom contribution to PP was highly variable, ranging
577 from <10% to ~100% depending on the bloom stage; but even when *Phaeocystis* appeared to be
578 favored, diatoms still had a significant (~50%) contribution to PP. While there was agreement
579 with previous regional studies regarding the rate of diatom cellular export, we observed
580 significantly elevated bSiO_2 export. Such a discrepancy can be resolved if a higher fraction of the
581 diatom material exported during our study was modified by zooplankton grazers, relative to
582 previous studies, or if much of this bSiO_2 was derived from melting ice and/or advection.

583

584 *Data availability.* All data are available upon request to the authors or are available through the
585 UiT research data bank (<https://dataverse.no/dataverse/uit>).

586

587 *Author contributions.* JK, CMD, SA conceived/designed the study and conducted analysis. JK,
588 CMD, IM, PA, MFM, IW, SA conducted the fieldwork. PW and SK conducted analysis. All co-
589 authors contributed to the writing of the paper, led by JK.

590

591 *Competing interests.* The authors declare that they have no conflict of interest.

592



593 *Acknowledgments.* The authors thank the science party and crew of the RV *Helmer Hanssen*. We
594 also thank S. Øygarden, E. Kube, A. Renner, D. Vogedes, H. Foshaug, S. Acton, D. Wiik, B. Vaaja
595 and W. Dobbins for logistic support. Primary data analysis was supported by the Dauphin Island
596 Sea Lab. Vessel time, ancillary data and I. Wiedmann's and P. Wassmann's contribution was
597 supported by ARCEX, funded by industry partners and the Research Council of Norway (project
598 #228107). P. Assmy was supported by the Research Council of Norway (project no. 244646) and
599 M. Fernández-Méndez by the Ministry of Foreign Affairs, Norway (project ID Arctic). J. Krause,
600 C. Duarte, and S. Agustí were supported by internal funding sources at their respective institutions.
601

602 **References**

- 603 Allen, J. T., Brown, L., Sanders, R., Moore, C. M., Mustard, A., Fielding, S., Lucas, M., Rixen, M.,
604 Savidge, G., and Henson, S.: Diatom carbon export enhanced by silicate upwelling in the northeast
605 Atlantic, *Nature*, 437, 728, 2005.
- 606 Anderson, L., and Dryssen, D.: Chemical-constituents of the arctic ocean in the svalbard area,
607 *Oceanologica Acta*, 4, 305-311, 1981.
- 608 Arrigo, K. R., van Dijken, G., and Pabi, S.: Impact of a shrinking Arctic ice cover on marine primary
609 production, *Geophysical Research Letters*, 35, 2008.
- 610 Assmy, P., Fernández-Méndez, M., Duarte, P., Meyer, A., Randelhoff, A., Mundy, C. J., Olsen, L. M.,
611 Kauko, H. M., Bailey, A., and Chierici, M.: Leads in Arctic pack ice enable early phytoplankton
612 blooms below snow-covered sea ice, *Scientific reports*, 7, 40850, 2017.
- 613 Banahan, S., and Goering, J. J.: The production of biogenic silica and its accumulation on the
614 southeastern Bering Sea shelf, *Continental Shelf Research*, 5, 199-213, 1986.
- 615 Bauerfeind, E., Nöthig, E.-M., Beszczynska, A., Fahl, K., Kaleschke, L., Kreker, K., Klages, M.,
616 Soltwedel, T., Lorenzen, C., and Wegner, J.: Particle sedimentation patterns in the eastern Fram Strait
617 during 2000–2005: Results from the Arctic long-term observatory HAUSGARTEN, *Deep Sea
618 Research Part I*, 56, 1471-1487, 2009.
- 619 Bidle, K. D., Manganelli, M., and Azam, F.: Regulation of oceanic silicon and carbon preservation by
620 temperature control on bacteria, *Science*, 298, 1980-1984, 2002.
- 621 Brown, L., Sanders, R., Savidge, G., and Lucas, C. H.: The uptake of silica during the spring bloom in the
622 Northeast Atlantic Ocean, *Limnology and Oceanography*, 48, 1831-1845, 2003.
- 623 Brzezinski, M. A.: The Si:C:N ratio of marine diatoms: Interspecific variability and the effect of some
624 environmental variables, *Journal of Phycology*, 21, 347-357, 1985.
- 625 Brzezinski, M. A., Phillips, D. R., Chavez, F. P., Friederich, G. E., and Dugdale, R. C.: Silica production
626 in the Monterey, California, upwelling system, *Limnology and Oceanography*, 42, 1694-1705, 1997.
- 627 Brzezinski, M. A., Nelson, D. M., Franck, V. M., and Sigmon, D. E.: Silicon dynamics within an intense
628 open-ocean diatom bloom in the Pacific sector of the Southern Ocean, *Deep-Sea Research II*, 48,
629 3997-4018, 2001.
- 630 Brzezinski, M. A., Pride, C. J., Franck, V. M., Sigman, D. M., Sarmiento, J. L., Matsumoto, K., Gruber,
631 N., Rau, G. H., and Coale, K. H.: A switch from Si (OH) 4 to NO₃⁻ depletion in the glacial Southern
632 Ocean, *Geophysical research letters*, 29, 2002.
- 633 Coello-Camba, A., Agustí, S., Vaqué, D., Holding, J., Arrieta, J. M., Wassmann, P., and Duarte, C. M.:
634 Experimental assessment of temperature thresholds for Arctic phytoplankton communities, *Estuaries
635 and coasts*, 38, 873-885, 2015.
- 636 Degerlund, M., and Eilertsen, H. C.: Main species characteristics of phytoplankton spring blooms in NE
637 Atlantic and Arctic waters (68–80 N), *Estuaries and coasts*, 33, 242-269, 2010.
- 638 DeMaster, D. J.: The accumulation and cycling of biogenic silica in the Southern Ocean: revisiting the
639 marine silica budget, *Deep-Sea Research II*, 49, 3155-3167, 2002.
- 640 Dugdale, R. C., Wilkerson, F. P., and Minas, H. J.: The role of a silicate pump in driving new production,
641 *Deep-Sea Research II*, 42, 697-719, 1995.



- 642 Egge, J., and Aksnes, D.: Silicate as regulating nutrient in phytoplankton competition, *Marine ecology*
643 *progress series*. Oldendorf, 83, 281-289, 1992.
- 644 Fripiat, F., Leblanc, K., Elskens, M., Cavagna, A.-J., Armand, L., André, L., Dehairs, F., and Cardinal,
645 D.: Efficient silicon recycling in summer in both the Polar Frontal and Subantarctic Zones of the
646 Southern Ocean, *Marine Ecology Progress Series*, 435, 47-61, 2011.
- 647 Hátún, H., Azetsu-Scott, K., Somavilla, R., Rey, F., Johnson, C., Mathis, M., Mikolajewicz, U., Coupel,
648 P., Tremblay, J.-É., and Hartman, S.: The subpolar gyre regulates silicate concentrations in the North
649 Atlantic, *Scientific reports*, 7, 14576, 2017.
- 650 Heiskanen, A.-S., and Keck, A.: Distribution and sinking rates of phytoplankton, detritus, and particulate
651 biogenic silica in the Laptev Sea and Lena River (Arctic Siberia), *Mar. Chem.*, 53, 229-245, 1996.
- 652 Hodal, H., Falk-Petersen, S., Hop, H., Kristiansen, S., and Reigstad, M.: Spring bloom dynamics in
653 Kongsfjorden, Svalbard: nutrients, phytoplankton, protozoans and primary production, *Polar Biology*,
654 35, 191-203, 2012.
- 655 Holding, J., Duarte, C., Sanz-Martín, M., Mesa, E., Arrieta, J., Chierici, M., Hendriks, I., García-Corral,
656 L., Regaudie-de-Gioux, A., and Delgado, A.: Temperature dependence of CO₂-enhanced primary
657 production in the European Arctic Ocean, *Nature Climate Change*, 2015.
- 658 Holm-Hansen, O., and Rieman, B.: Chlorophyll a determination: improvements in methodology, *Oikos*,
659 438-447, 1978.
- 660 Hoppe, C., Schuback, N., Semeniuk, D., Giesbrecht, K., Mol, J., Thomas, H., Maldonado, M., Rost, B.,
661 Varela, D., and Tortell, P.: Resistance of Arctic phytoplankton to ocean acidification and enhanced
662 irradiance, *Polar Biology*, 41, 399-413, 2018.
- 663 Hulth, S., Hall, P. O., Landén, A., and Blackburn, T.: Arctic sediments (Svalbard): pore water and solid
664 phase distributions of C, N, P and Si, *Polar Biology*, 16, 447-462, 1996.
- 665 Krause, J. W., Nelson, D. M., and Lomas, M. W.: Biogeochemical responses to late-winter storms in the
666 Sargasso Sea, II: Increased rates of biogenic silica production and export, *Deep-Sea Research I*, 56,
667 861-874, 10.1016/j.dsr.2009.01.002, 2009.
- 668 Krause, J. W., Brzezinski, M. A., and Jones, J. L.: Application of low level beta counting of ³²Si for the
669 measurement of silica production rates in aquatic environments, *Mar. Chem.*, 127, 40-47,
670 10.1016/j.marchem.2011.07.001, 2011.
- 671 Krause, J. W., Brzezinski, M. A., Villareal, T. A., and Wilson, C.: Increased kinetic efficiency for silicic
672 acid uptake as a driver of summer diatom blooms in the North Pacific Subtropical Gyre, *Limnology*
673 *and Oceanography*, 57, 1084-1098, 10.4319/lo.2012.57.4.1084, 2012.
- 674 Krause, J. W., Brzezinski, M. A., Villareal, T. A., and Wilson, C.: Biogenic silica cycling during summer
675 phytoplankton blooms in the North Pacific subtropical gyre, *Deep-Sea Research I*, 71, 49-60,
676 10.1016/j.dsr.2012.09.002, 2013.
- 677 Kristiansen, S., Farbot, T., and Naustvoll, L. J.: Production of biogenic silica by spring diatoms,
678 *Limnology and Oceanography*, 45, 472-478, 2000.
- 679 Kristiansen, S., Farbot, T., and Naustvoll, L.-J.: Spring bloom nutrient dynamics in the Oslofjord, *Marine*
680 *Ecology Progress Series*, 219, 41-49, 2001.
- 681 Kristiansen, S., and Hoell, E. E.: The importance of silicon for marine production, in: *Sustainable*
682 *Increase of Marine Harvesting: Fundamental Mechanisms and New Concepts*, Springer, 21-31, 2002.
- 683 Lalande, C., Bauerfeind, E., Nöthig, E.-M., and Beszczynska-Möller, A.: Impact of a warm anomaly on
684 export fluxes of biogenic matter in the eastern Fram Strait, *Progress in Oceanography*, 109, 70-77,
685 2013.
- 686 Lalande, C., Moriceau, B., Leynaert, A., and Morata, N.: Spatial and temporal variability in export fluxes
687 of biogenic matter in Kongsfjorden, *Polar Biology*, 39, 1725-1738, 2016.
- 688 Lasternas, S., and Agustí, S.: Phytoplankton community structure during the record Arctic ice-melting of
689 summer 2007, *Polar Biology*, 33, 1709-1717, 2010.
- 690 Leynaert, A., Nelson, D. M., Queguiner, B., and Tréguer, P.: The silica cycle in the Antarctic Ocean: Is
691 the Weddell Sea atypical?, *Marine ecology progress series*. Oldendorf [MAR. ECOL. PROG. SER.],
692 Vol., 96, 1-15, 1993.



- 693 Li, W. K., McLaughlin, F. A., Lovejoy, C., and Carmack, E. C.: Smallest algae thrive as the Arctic Ocean
694 freshens, *Science*, 326, 539-539, 2009.
- 695 Lomas, M. W., Moran, S. B., Casey, J. R., Bell, D. W., Tiahlo, M., Whitefield, J., Kelly, R. P., Mathis, J.
696 T., and Cokelet, E. D.: Spatial and seasonal variability of primary production on the Eastern Bering
697 Sea shelf, *Deep-Sea Research II*, 65-70, 126-140, 10.1016/j.dsr2.2012.02.010, 2012.
- 698 Martin-Jézéquel, V., Hildebrand, M., and Brzezinski, M. A.: Silicon metabolism in diatoms: Implications
699 for growth, *Journal of Phycology*, 36, 821-840, 2000.
- 700 Nelson, D. M., and Gordon, L. I.: Production and Pelagic Dissolution of Biogenic Silica in the Southern
701 Ocean, *Geochimica et Cosmochimica Acta*. Vol., 46, 491-501, 1982.
- 702 Nöthig, E.-M., Bracher, A., Engel, A., Metfies, K., Niehoff, B., Peeken, I., Bauerfeind, E., Cherkasheva,
703 A., Gäbler-Schwarz, S., and Hardge, K.: Summertime plankton ecology in Fram Strait-a compilation
704 of long-and short-term observations, *Polar Research*, 34, 2015.
- 705 Oziel, L., Neukermans, G., Ardyna, M., Lancelot, C., Tison, J. L., Wassmann, P., Sirven, J., Ruiz-Pino,
706 D., and Gascard, J.-C.: Role for Atlantic inflows and sea ice loss on shifting phytoplankton blooms in
707 the Barents Sea, *Journal of Geophysical Research: Oceans*, 2017.
- 708 Paasche, E.: Growth of the plankton diatom *Thalassiosira nordenskiöldii* Cleve at low silicate
709 concentrations, *Journal of Experimental Marine Biology and Ecology*, 18, 173-183, 1975.
- 710 Paasche, E., and Ostergren, I.: The annual cycle of plankton diatom growth and silica production in the
711 inner Oslofjord I, *Limnology and Oceanography*, 25, 481-494, 1980.
- 712 Rat'kova, T. N., and Wassmann, P.: Seasonal variation and spatial distribution of phyto-and
713 protozooplankton in the central Barents Sea, *Journal of Marine Systems*, 38, 47-75, 2002.
- 714 Reigstad, M., Wassmann, P., Riser, C. W., Øygarden, S., and Rey, F.: Variations in hydrography,
715 nutrients and chlorophyll a in the marginal ice-zone and the central Barents Sea, *Journal of Marine
716 Systems*, 38, 9-29, 2002.
- 717 Rey, F., Skjoldal, H. R., and Hassel, A.: Seasonal development of plankton in the Barents Sea: a
718 conceptual model, *ICES Symposium* 56, 1987,
- 719 Rey, F.: Declining silicate concentrations in the Norwegian and Barents Seas, *ICES Journal of Marine
720 Science*, 69, 208-212, 2012.
- 721 Sakshaug, E.: Primary and secondary production in the Arctic Seas, in: *The organic carbon cycle in the
722 Arctic Ocean*, Springer, 57-81, 2004.
- 723 Slagstad, D., and Støle-Hansen, K.: Dynamics of plankton growth in the Barents Sea: model studies,
724 *Polar Research*, 10, 173-186, 1991.
- 725 Steemann Nielsen, E.: The use of radio-active carbon (C14) for measuring organic production in the sea,
726 *Journal de Conseil*, 18, 117-140, 1952.
- 727 Torres-Valdés, S., Tsubouchi, T., Bacon, S., Naveira-Garabato, A. C., Sanders, R., McLaughlin, F. A.,
728 Petrie, B., Kattner, G., Azetsu-Scott, K., and Whitley, T. E.: Export of nutrients from the Arctic
729 Ocean, *Journal of Geophysical Research: Oceans*, 118, 1625-1644, 2013.
- 730 Tréguer, P., Bowler, C., Moriceau, B., Dutkiewicz, S., Gehlen, M., Aumont, O., Bittner, L., Dugdale, R.,
731 Finkel, Z., and Iudicone, D.: Influence of diatom diversity on the ocean biological carbon pump,
732 *Nature Geoscience*, 11, 27, 2018.
- 733 Tréguer, P. J., and De La Rocha, C. L.: The World Ocean Silica Cycle, in: *Annual Review of Marine
734 Science*, Vol 5, Annual Review of Marine Science, 477-501, 2013.
- 735 Tremblay, J.-E., Gratton, Y., Fauchot, J., and Price, N. M.: Climatic and oceanic forcing of new, net, and
736 diatom production in the North Water, *Deep Sea Research Part II: Topical Studies in Oceanography*,
737 49, 4927-4946, 2002.
- 738 Tremblay, J.-É., and Gagnon, J.: The effects of irradiance and nutrient supply on the productivity of
739 Arctic waters: a perspective on climate change, in: *Influence of climate change on the changing
740 Arctic and sub-Arctic conditions*, Springer, 73-93, 2009.
- 741 Tsuji, T., and Yanagita, T.: Improved fluorescent microscopy for measuring the standing stock of
742 phytoplankton including fragile components, *Marine Biology*, 64, 207-211, 1981.



- 743 Utermöhl, H.: Zur Vervollkommung der quantitativen phytoplankton-methodik, *Mitteilungen*
744 *Internationale Vereinigung für Theoretische und Angewandte Limnologie*, 9, 38, 1958.
- 745 Vaquer-Sunyer, R., Duarte, C. M., Regaudie-de-Gioux, A., Holding, J., García-Corral, L. S., Reigstad,
746 M., and Wassmann, P.: Seasonal patterns in Arctic planktonic metabolism (Fram Strait-Svalbard
747 region), *Biogeosciences*, 10, 1451–1469, 10.5194/bg-10-1451-2013, 2013.
- 748 Varela, D. E., Crawford, D. W., Wrohan, I. A., Wyatt, S. N., and Carmack, E. C.: Pelagic primary
749 productivity and upper ocean nutrient dynamics across Subarctic and Arctic Seas, *Journal of*
750 *Geophysical Research: Oceans*, 118, 7132–7152, 2013.
- 751 Wassmann, P., Ratkova, T., Andreassen, I., Vernet, M., Pedersen, G., and Rey, F.: Spring bloom
752 development in the marginal ice zone and the central Barents Sea, *Marine Ecology*, 20, 321–346,
753 1999.
- 754 Wassmann, P., Slagstad, D., Riser, C. W., and Reigstad, M.: Modelling the ecosystem dynamics of the
755 Barents Sea including the marginal ice zone: II. Carbon flux and interannual variability, *Journal of*
756 *Marine Systems*, 59, 1–24, 2006.
- 757 Wassmann, P., Slagstad, D., and Ellingsen, I.: Primary production and climatic variability in the
758 European sector of the Arctic Ocean prior to 2007: preliminary results, *Polar Biology*, 33, 1641–1650,
759 2010.
- 760 Wexels Riser, C., Wassmann, P., Olli, K., Pasternak, A., and Arashkevich, E.: Seasonal variation in
761 production, retention and export of zooplankton faecal pellets in the marginal ice zone and central
762 Barents Sea, *Journal of Marine Systems*, 38, 175–188, 2002.
- 763 Wiedmann, I., Reigstad, M., Sundfjord, A., and Basedow, S.: Potential drivers of sinking particle's size
764 spectra and vertical flux of particulate organic carbon (POC): Turbulence, phytoplankton, and
765 zooplankton, *Journal of Geophysical Research: Oceans*, 119, 6900–6917, 2014.



766 Table 1 – Station properties including surface temperature, nutrients and chlorophyll a (\pm standard deviation), 20-m biogenic silica stock (\int bSiO₂),
 767 production (\int ρ) and depth-weighted specific production (V_{AVE}), 40-m integrated diatom abundance (\int Diatom) and export of bSiO₂ and diatoms at
 768 40 m. The disparity between the integration depths for bSiO₂ standing stock and diatom abundance reflects the lack of bSiO₂ samples to 40 m
 769 depth and that the latter are used to compare with diatom export (Discussion). Note: Hinlopen (ice) station not included. The Polar Front \int Diatom
 770 is the mean of two profiles.

Station Name	T (°C)	[NO ₃ + NO ₂] (μ M)	[Si(OH) ₄] (μ M)	[Chl <i>a</i>] (μ g L ⁻¹)	20-m \int bSiO ₂ (mmol Si m ⁻²)	20-m \int ρ (mmol Si m ⁻² d ⁻¹)	20-m V_{AVE} (d ⁻¹)	40-m \int Diatom abundance (10 ⁹ cells m ⁻²)	40-m bSiO ₂ export (mmol Si m ⁻² d ⁻¹)	40-m Diatom export (10 ⁶ cells m ⁻² d ⁻¹)
‡van Mijenfjorden	-0.43	8.1	3.8	1.84 \pm 0.19	10.8	-	-	7.67	9.03	769
‡Bredjupet	4.72	9.4	4.5	0.72 \pm 0.03	1.9	0.27	0.13	-	-	-
Bellsund Hula	0.69	<0.1	0.5	2.66 \pm 0.05	15.3	0.49	0.06	-	-	-
Hornsund	-0.28	1.6	1.1	2.50 \pm 0.20	-	-	-	8.97	-	1180
‡Hornsunddjupet	-0.20	<0.1	0.4	2.43 \pm 0.17	42.2	1.46	0.03	-	-	-
‡Edgeøya	-0.70	0	0.7	1.99 \pm 0.03	-	-	-	-	-	-
‡Erik Erikssenstretet	-1.58	0.4	0.4	4.77 \pm 0.31	34.9	1.03	0.04	252	4.00	436
‡*Polar Front Station	2.19	<0.1	1.1	3.00 \pm 0.03	-	-	-	527	-	-
Atlantic	4.10	3.3	1.4	6.66 \pm 0.33	-	-	-	-	9.20	2380

771 †Surface value

772 *25 m depth

773 ‡Denotes concurrent primary production and biogenic silica production measurements at one depth

774

775

776

777



778 Figure Captions:

779

780 Figure 1: Surface properties during 2016 ARCEX cruise including A) Nitrate + Nitrite (μM), B) dissolved
781 silicic acid (μM), C) biogenic silica ($\mu\text{mol Si L}^{-1}$), D) Chlorophyll *a* ($\mu\text{g L}^{-1}$) and E) Temperature ($^{\circ}\text{C}$)
782 overlaid on station map. Station names are denoted on the map and colored arrows generalize the flow of
783 Atlantic-influenced (red) and Arctic-influenced (blue) waters.

784

785 Figure 2: Vertical profiles for A) dissolved silicic acid, B) Nitrate + Nitrite, C) biogenic silica standing
786 stock, D) biogenic silica production rate, and E) biogenic silica export. Symbols are associated by station,
787 and line connectors are used to denote profile data opposed to individual symbols noting samples at one
788 depth.

789 Figure 3: Diatom abundance (A) and assemblage composition (B–D) in the water column, and diatom
790 export (E) and assemblage composition (F–H) within sediment traps. Note – taxonomy information only
791 shown for stations where both water-column and sediment-trap data were available (see text for species).
792 Resting spores (e.g. *Chaetoceros*, *Thalassiosira*) were absent from the 40-m sediment traps; thus,
793 proportional abundances for spore-producing taxa are entirely for vegetative cells. For panel A, there are
794 replicate diatom abundance measurements (from separate hydrocasts) for the Polar Front station.

795

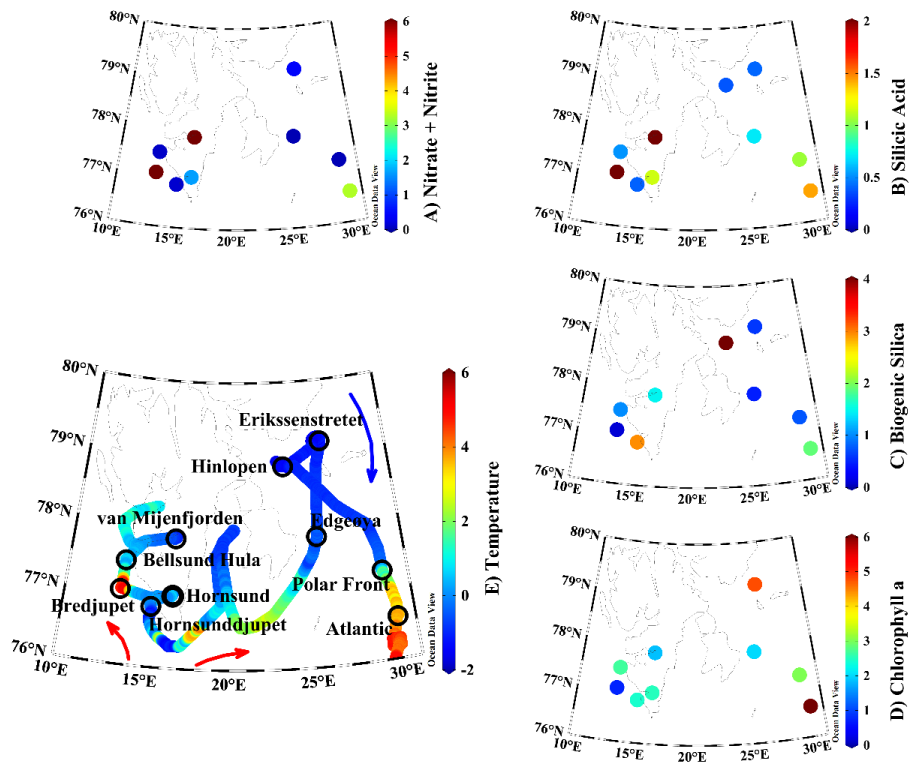
796 Figure 4: Assessment of Si uptake limitation by available silicic acid during ARCEX. A) 8-point kinetic
797 experiments taken at four stations (legend next to panel B). Data were fit to a Michaelis-Menten
798 hyperbola using SigmaPlot 12.3 software. B) Enh. ratio profiles (i.e. V_b in $+18.0 \mu\text{M} [\text{Si}(\text{OH})_4]$ treatment
799 relative to V_b in the ambient $[\text{Si}(\text{OH})_4]$ treatment) at four stations.

800 Figure 5: Diagnosis of potential silicon limitation for diatom production during ARCEX. A) Nitrate +
801 Nitrite drawdown as a function of dissolved silicic acid. B) The ratio of V_b at ambient $[\text{Si}(\text{OH})_4]$ to V_{max}
802 versus dissolved silicic acid. In both panels, linear regressions were done using a Model II reduced major
803 axis method. For comparison, the same relationship for the Sargasso Sea in the North Atlantic
804 subtropical gyre, as synthesized in Krause et al. (2012).

805



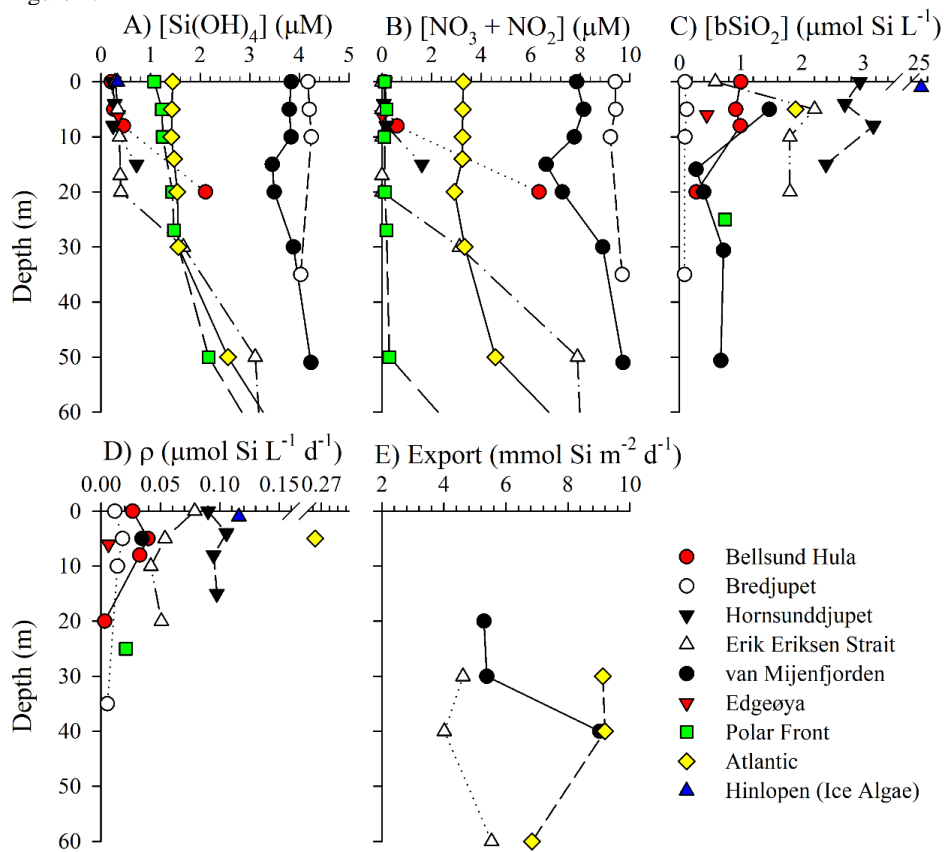
806 Figure 1:



807
808



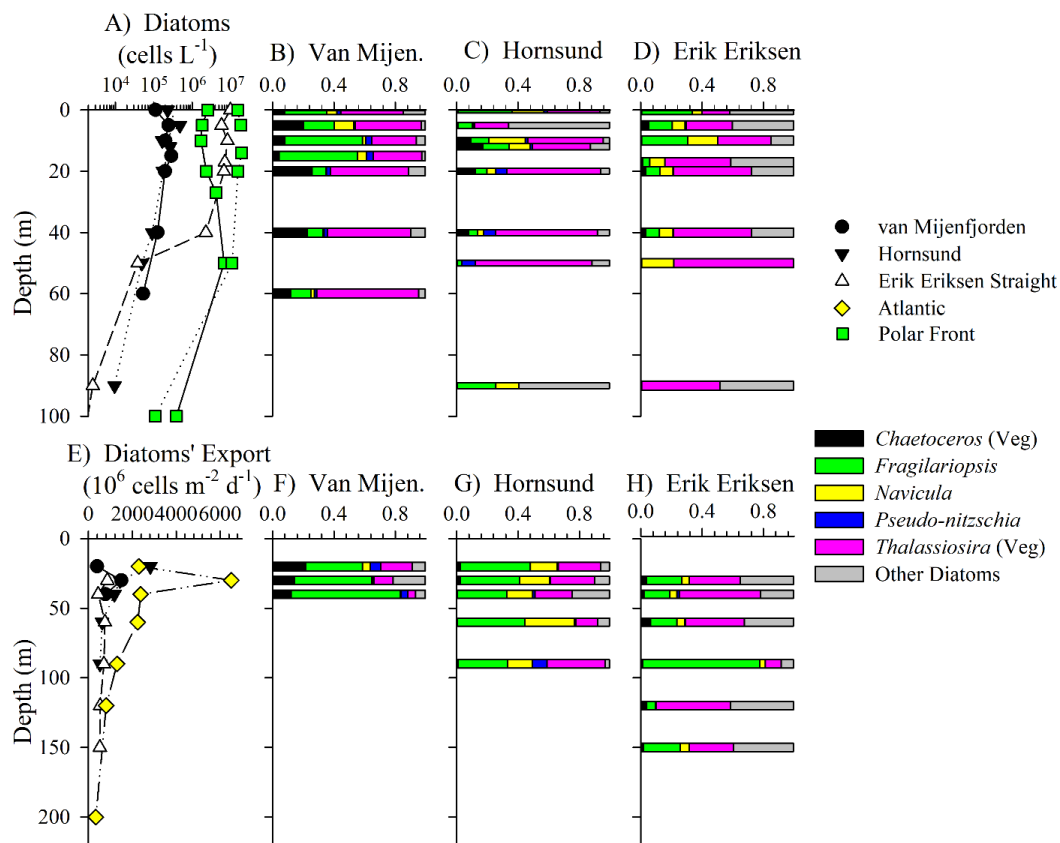
809 Figure 2:



810
 811



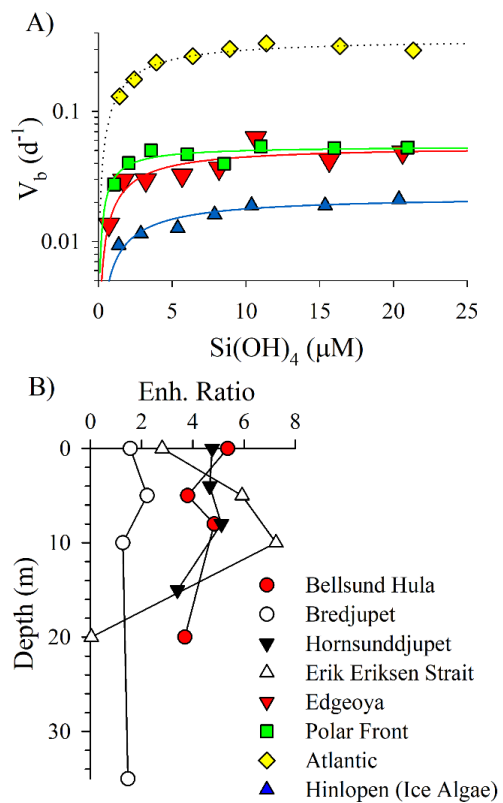
812 Figure 3:



813
814



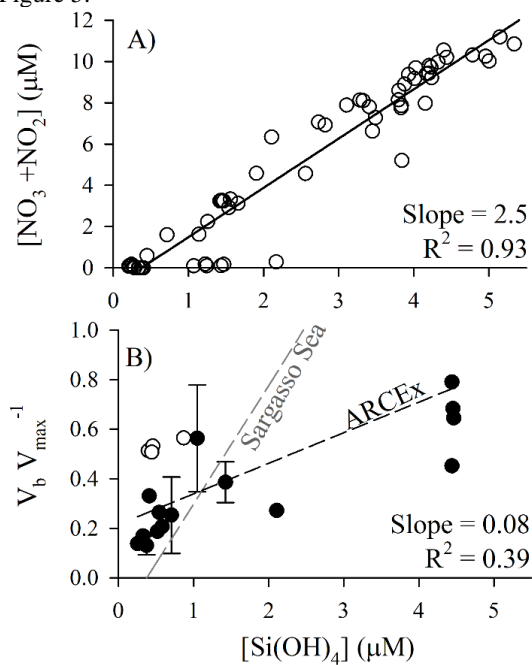
815 Figure 4:



816
817



818 Figure 5:



819